Performance Analysis of Ultrathin $Cu(In,Ga)Se_2$ Solar Cells with Backwall Superstrate Configuration Using AMPS-1D

Abdelhafid Mouhoub
Electronics Department, Amar Teliji University and
Laboratory of Electrochemical and Materials, Setif-1
University, Algeria
a.mouhoub@lagh-univ.dz

Fahima Khaled
Electronics Department
Mohamed El Bachir El Ibrahimi University
Bordj Bou Arreridj, Algeria
khaled_fahima@yahoo.fr

Abdessalem Bouloufa
Laboratory of Electrochemical and Materials
Setif-1 University
Setif, Algeria
a_bouloufa@yahoo.fr

Received: 17 September 2022 | Revised: 29 September 2022 | Accepted: 3 October 2022

Abstract-This study used AMPS-1D to peform numerical simulations and model the behavior of back-wall superstrate solar cells based on $Cu(In,Ga)Se_2$ (CIGS) thin films to investigate optimal conditions and obtain maximum efficiency. The effects of absorber thickness and density of interface defects were examined along with the work function of the transparent conductive oxide (W_{TCO}) to investigate their influence on the output parameters. Measurements of device performance (J-V) and Quantum Efficiency (QE) showed that the performance of the cell improved as the thickness of the CIGS layer decreased because photons were absorbed near the junction. The device achieved an efficiency of 16.4% using an optimal thickness for the CIGS layer on the order of 0.3µm, defect densities in the range of 10^{13}-$10^{15}cm^{-3}$, doping concentration of the n-TCO back contact on the order of $10^{19}cm^{-3}$, and W_{TCO} in the range of 4.5-5.2eV. These results show that the generated electron-hole pairs had a high probability of separation and demonstrate the potential of this device structure.

Keywords-$Cu(In,Ga)Se_2$; thin films solar cells; backwall superstrate; transparent conductive oxide; device modeling

I. INTRODUCTION

$Cu(In,Ga)Se_2$ (CIGS) is regarded as one of the most promising semiconductors for use in thin-film photovoltaic applications [1, 2], due to its sizeable optical coefficient in the range of the solar spectrum and its electrical and optical properties, which vary depending on the preparation condition and the production technique [3, 4]. The production of this semiconductor using various techniques and different types of substrates was examined in [5, 6]. Higher efficiency of CIGS thin film solar cells was achieved recently, with values exceeding 23.4%, from devices in the typical substrate cell configuration [1, 7], wherein the first step of device fabrication, the molybdenum layer was deposited as a back contact layer on Soda-Lime Glass (SLG), followed by the deposit of the p-CIGS absorber layer. Then, the n-type buffer layer grew on top of the CIGS to form the crucial p-n junction [8] that completes the structure of the solar cell. Next, a thin layer of high resistance intrinsic (i-ZnO) was applied to the front window, followed by a thin layer, to form the front electrode while ensuring the optimal transmission of solar spectrum photons. The device was finished by depositing the collecting grid [9] and illuminated through the TCO window layer [10, 11]. The best performances were obtained by depositing 20-50nm of the CdS buffer layer on top of the CIGS absorber layer, whose thickness was around 2-3µm [12-14]. The economic aspect remains critical in the industrial development of CIGS technology [14], and it is necessary to reduce its production cost. One of the drawbacks of this process remains the use of rare elements, such as Indium and Gallium [11, 12]. In this context, this study investigated the development of low-cost and environmentally friendly photovoltaic cells. Reducing the thickness of the CIGS has the eventual benefit of reducing costs, while fast fabrication and limiting the use of rare elements can achieve higher manufacturing throughput [15-17].

The back-wall superstrate configuration of CIGS photovoltaic devices has the potential for better light harvesting than the substrate cell structure [17-19]. In this structure, the manufacturing sequences are reversed concerning the substrate configuration. In the first step, the absorber layer is deposited onto the TCO window layer and illumination comes from the back region. Hence, a wide band gap transparent back contact is required in the structure [20]. In addition, the critical absorber buffer interdiffusion is restricted [1, 2]. This study focused on an original back-wall superstrate solar cell of the

Corresponding author: Abdelhafid Mouhoub

type SLG/n-SnO_2:F/p-CIGS/n-In_2Se_3/i-ZnO/Mo. The CIGS-based cell eliminates the need for transparent encapsulation due to the collection grids at both the cell and the module productions and the requirement for toxic cadmium sulfide (CdS) used in conventional cells [1]. Developing solar cells with high conversion efficiency and based on hetero-structures requires knowledge of the effects that limit their photovoltaic performance, in particular the phenomenon of diffusion and recombination at the interfaces and in the volume of the material of the different layers of the device.

The CIGS-based back-wall superstrate solar cell's behavior has been the subject of considerable theoretical modeling efforts in this area. This study investigates the main parameters likely to be involved in the optimization of the photovoltaic performance of the cells studied using AMPS-1D [21, 22], proposing indicative design parameters for the back-wall superstrate solar cell. Therefore, this study focuses on the investigation of the properties of the absorber layer with different thicknesses, densities of interface defects (N_{it}), and the TCO/absorber interface that may limit current transport in the cell, aiming to examine the limits of the device and determine the most favorable parameters. The best obtained efficiency was 16.4%, showing the prospects of this structure. The simulations results were found to be in good agreement with the values reported in [2] and allowed the verification of the proposed AMPS parameters. However, the main motive of this study was to examine the trends of device performance rather than predict optimum values.

II. DETAILS OF THE SIMULATED SOLAR CELL

The AMPS-1D software was used to evaluate the performance of the device as the design of the absorber layer varied. The numerical modeling of the semiconductor device was based on the simultaneous resolution of the Poisson and the continuity equations for the holes and electrons [23, 24]. AMPS-1D solves three coupled differential equations in suitable limit conditions and then evaluates the electrostatic potential and the quasi-Fermi level for holes and electrons at any point in the device [25, 26]. Once these variables are identified according to the depth, it is easy to evaluate the carrier concentrations, electric fields, current density-voltage characteristics (*J-V*), Quantum Efficiency (QE) curves, and the photovoltaic output parameters open-circuit voltage (V_{oc}), short-circuit current density (J_{sc}), fill factor (*FF*), and efficiency (η) [6]. These parameters describe the performance of solar cells [25, 27]. Modeling solar cells has the advantage that all device and material properties are well restricted as they are input parameters of the model. Therefore, trend assessment and quantified changes in *J-V* or *QE* measurements are probable.

The chosen back-wall solar cell structure consists of a stack of thin layers: SLG/SnO_2:F/p-CIGS/n-In_2Se_3/i-ZnO/Mo. The TCO layer is required to form the front electrode while ensuring the optimal transmission of the solar spectrum photons. SnO_2 was chosen for its excellent conductivity, as it is a wide-gap semiconductor [28]. The thin layer of In_2Se_3 was deposited on the CIGS absorber layer, which is involved in the formation of the p-n junction and also protects the surface of the CIGS. Figure 1 shows the proposed CIGS solar cell. The interface recombination velocities were fixed at 10^7cm/s and the light reflection of the rear and the front contacts were assumed to be 1 and 0.1 respectively. AM 1.5D solar radiation was used as the illumination source, corresponding to a power of 1000W/m^2. The electrical and optical properties of the CIGS layer were incorporated using the close-spaced vapor transport technique [21]. Table I shows the parameters of each semiconductor of the typical cell used in the simulation, as reported in the literature.

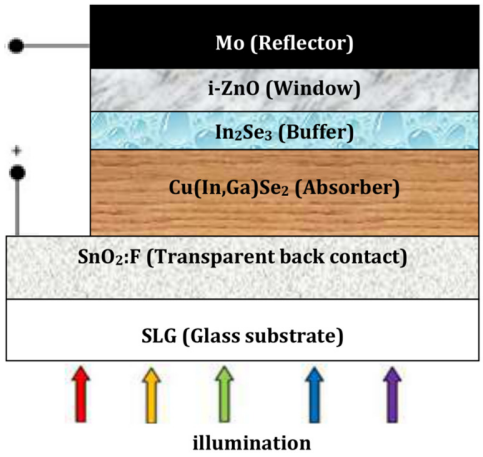

Fig. 1. Basic structures of back-wall superstrate device.

TABLE I. BASELINE PARAMETERS USED FOR THE BACKWALL SUPERSTRATE CIGS SOLAR CELLS IN THE SIMULATIONS

Parameters	i-ZnO	In_2Se_3	CIGS	SnO_2:F
Layer thickness: *d* (nm)	50	50	variable	300
Dielectric constant: ε_r	9	10	13.6	9
Effective conduction band density: N_C (cm^{-3})	2.2×10^{18}	2.2×10^{18}	2.2×10^{18}	2.2×10^{18}
Effective valence band density: N_V (cm^{-3})	1.8×10^{19}	1.8×10^{19}	1.8×10^{19}	1.8×10^{19}
Doping concentration: (N_A) (cm^{-3})	/	/	2×10^{16}	/
Doping concentration: (N_D) (cm^{-3})	1×10^{14}	1×10^{16}	/	1×10^{19}
Band gap: E_g (eV)	3.30	2.40	1.20	3.6
Electron affinity: χ (eV)	4.00	3.80	4.10	4.00
Electron mobility: μ_e (cm^2/V.s)	100	50	50	100
Hole mobility: μ_h (cm^2/V.s)	25	12	12	25
Defect density: N_{DG}/N_{AG} (cm^{-3})	1.5×10^{14}	1.5×10^{17}	1×10^{12}	1.5×10^{14}
Capture cross-section electrons: σ_e (cm^2)	1×10^{-13}	1×10^{-17}	1×10^{-13}	1×10^{-13}
Capture cross-section holes: σ_h (cm^2)	1×10^{-15}	1×10^{-12}	1×10^{-15}	1×10^{-15}

III. RESULTS AND DISCUSSION

A. Effect of the CIGS Absorber Layer Thickness

Several studies focused on reducing the thickness of the absorber layer without affecting solar cell performance. A simulation of the *J-V* characteristic was obtained by varying the thickness of the p-CIGS layer in the structure between 0.05 and 2µm to obtain the optimal results for the back-wall superstrate configuration cells. Figure 2 shows the variation of the current density as a function of the bias voltage for different thicknesses of the absorber layer.

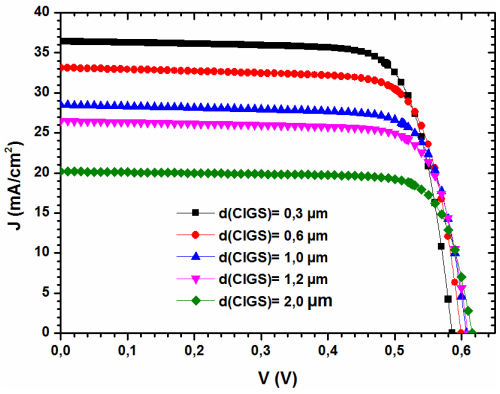

Fig. 2. Current-voltage characteristics of the solar cell with different thicknesses of CIGS absorber.

The absorber's thickness significantly influences the performance of the photovoltaic cell. The results showed that the variation and reduction of d(CIGS) from 2 to 0.3µm lead to an increase of J_{sc} from 20.19 to 36.42mA/cm^2. This means that the power provided by the cell increases as the thickness of the CIGS layer decreases and the efficiency is lost due to the parasitic losses, including higher series resistance. The thickness of the CIGS layer affects the quantum efficiency of the solar cell, as shown in Figure 3, and the active layer affects the short wavelength. For the thick absorber layer, the photo-generation process is produced far from the back contact region and, therefore, not near the electric field of the space charge region (ZCE).

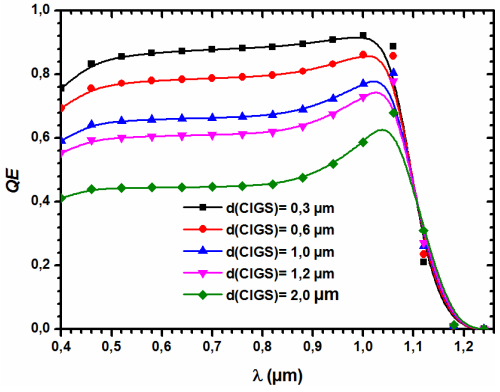

Fig. 3. The quantum efficiency of the device with different absorber thicknesses.

The generation probability in a thin absorber less than 0.5µm is very high and, therefore, produces photocarriers close to the electric field. This is partly due to a considerable absorption loss in the rear region of the CIGS absorber layer. Another probable explanation is that the diffusion length of the minority carrier layer in a thinner absorber layer is similar to its thickness. As a result, $QE(\lambda)$ at a short wavelength is improved without a significant decrease in efficiency, and the parasitic absorption in the buffer layer is prevented, as shown in Figure 3. The optimal absorber layer thickness was approximately 0.25-0.5µm in this case, which reduces the thickness of the absorber layer and has the eventual benefit of reducing the cost of manufacture due to the reduced material usage.

B. Effect of Absorber Thickness on Photovoltaic Parameters

Figure 4 illustrates the influence of the thickness of the CIGS on the photovoltaic parameters of the cell (J_{sc}, V_{oc}, FF, and η). It can be noted that the voltage V_{oc} is practically constant when reducing the thickness of the p-CIGS absorber layer from 2 to 0.25µm. The current density of J_{sc} strongly depends on the thickness of the p-CIGS absorber, and it increases with decreasing thickness. The efficiency of cell structure also increases rapidly because the photons are absorbed close to the p-CIGS/n-In_2Se_3 junction and the generated photocarriers have a high probability of being separated. For absorber thickness greater than 0.5µm, the photons are absorbed away from the electric field, so that V_{oc} and J_{sc} decrease as the thickness of the absorber increases up to 2µm. Reducing V_{oc} and J_{sc} results in a reduction in conversion efficiency (η). This is probably due to imperfections in the thick absorber, which allowed the emergence of many defects. When the absorber thickness is reduced below 0.25µm, the performance of the device begins to deteriorate due to incomplete optical absorption. A maximum cell conversion efficiency of 16.4% was obtained for a thickness in the range of 0.25 to 0.5µm for the CIGS absorber.

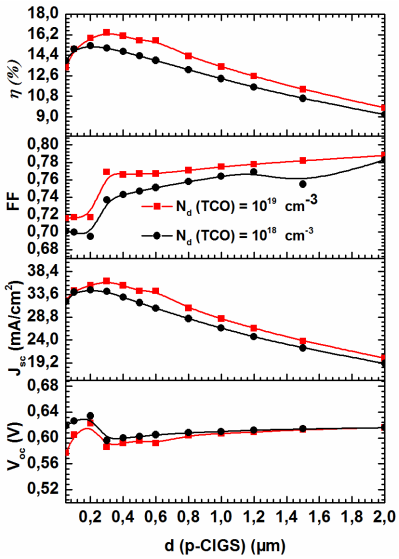

Fig. 4. The dependence of solar cell performance on CIGS thickness with deferent N_d(TCO).

C. Effect of the Density of Defects N_{it} of the Absorber Layer on the Performance of the Cell

Figure 5 shows the effect of the concentration of the absorber layer defects on the photovoltaic parameters (J_{sc}, V_{oc}, FF, and η) with various doping concentrations of the TCO layer. The results showed that high efficiency is achieved when the defect density is in the range of 10^{12} to 10^{15}cm^{-3}, because the barrier that causes the recombination is not produced at the CIGS/In_2Se_3 interface, and J_{sc}, V_{oc}, FF, and η are practically constant. On the other hand, when the concentration of the

absorber layer defects is more significant than 10^{15}cm^{-3}, the variation of V_{oc}, J_{sc}, and FF becomes very significant, affecting the cell's performance. These parameters decrease sharply as a result of the formation of a barrier in the face of the photogenerated electrons. A strongly doped layer of TCO is also preferred to shove the electrons photogenerated inward the bulk of the absorber.

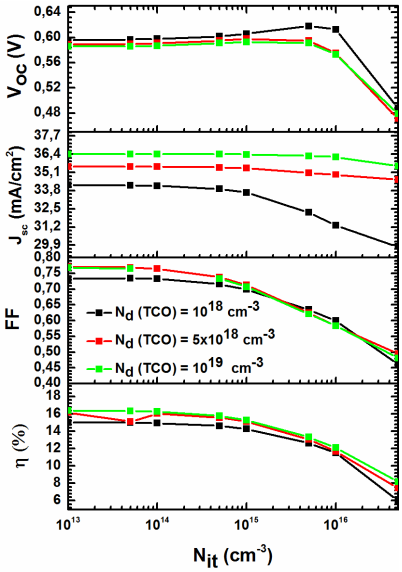

Fig. 5. The photovoltaic parameters as a function of CIGS density defect with deferent N_d(TCO).

D. Effect of the Back TCO/CIGS Contact Region

The development of a high-quality TCO back-contact while maintaining the efficiency of light transmission throughout the top CIGS layer is essential to obtain a high efficiency of the back-wall solar cells. The TCO work function *(W_{TCO})* of the back contact region was a means factor in affecting the back-wall solar cell performance. Figure 6 shows the dependence of the performance of the SnO_2:F/p-CIGS/n-In_2Se_3/i-ZnO/Mo solar cell on the variation of W_{TCO}. It can be seen that V_{oc}, FF, and η increase with W_{TCO} of the back SLG/SnO_2:F/p-CIGS surface. It is necessary to use a suitable work function of the back TCO to have ohmic contact in the back contact and reduce the barrier recombination. Furthermore, when W_{TCO} is higher than 5.2eV, the potential barriers of the TCO/p-CIGS Schottky contact are effectively elevated than the crucial n-In_2Se_3/p-CIGS junction and the TCO/p-CIGS contact, and the p-CIGS/n-In_2Se_3 junction will have potential barriers on the contrary course of action. In that event, overlapping the space charge region involving the two junctions would induce a drop in the device performance. The back contact resistance depends on the barrier potential (Φ_b) and N_d(TCO). A low height barrier (Φ_b) and a high concentration of N_d are needed to have low resistance and ohmic contacts and avoid the depletion zone created at the TCO/CIGS interface. The simulation results confirm that the N_d (TCO) is required to be in the range of 10^{19}cm^{-3}, to obtain high performance and induce the increase of the $QE(\lambda)$, as shown in Figure 7, due to the decrease of recombination at the TCO/CIGS interface.

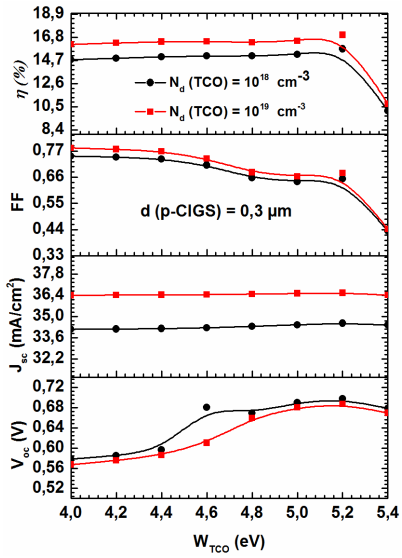

Fig. 6. The dependence of solar cell performance on W_{TCO} with deferent N_d(TCO).

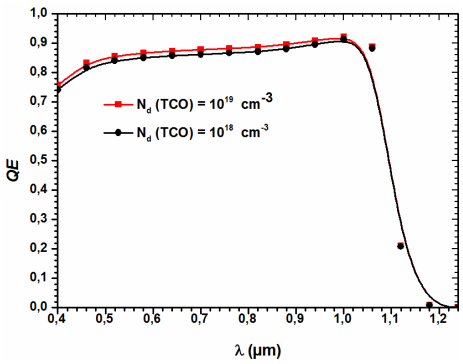

Fig. 7. The dependence of the quantum efficiency on the N_d(TCO).

IV. CONCLUSIONS

This study investigated the performance of back-wall superstrate solar cells using AMPS-1D software with a modified absorber layer. Based on the results, the thickness of the absorber layer, the densities of interface defects (N_{it}), and the work function of the back transparent conductive oxide on the performance of the CIGS back-wall superstrate cell structure. To improve conversion efficiency, the CIGS absorber thickness must be thinner as possible (0.25µm-0.5µm), because the photons will be captured in the area of the junction, and the generated electron-hole pairs will have a high probability of being split apart because there will be a gap between them. However, the results of the simulation demonstrated that even a high density of defects does not prevent a structure from achieving exceptional levels of performance. The N_{it} of the absorber layer was in the range of 10^{12}-10^{15}cm^{-3}. The optimized conditions were the doping concentration of the n-TCO back contact N_d on the order of 10^{19}cm^{-3} and W_{TCO} between 4.6-5.2eV. The CIGS back-wall superstrate solar cell with an absorber layer thickness of 0.3µm showed the best efficiency of 16.4%.

ACKNOWLEDGMENT

The authors express their gratitude to Dr. S.J. Fonash of the Pennsylvania State University for developing AMPS-1D, which was used in this study.

REFERENCES

[1] M. Ni, J. M. Liu, Z. Q. Li, Q. Shen, Y. Z. Feng, and X. D. Feng, "Simulation of graded bandgap on backwall superstrate CIGS solar cells with MoOx electron reflection layer," *Materials Research Express*, vol. 6, no. 11, Jul. 2019, Art. no. 116441, https://doi.org/10.1088/2053-1591/ab4c5c.

[2] J. K. Larsen, H. Simchi, P. Xin, K. Kim, and W. N. Shafarman, "Backwall superstrate configuration for ultrathin Cu(In,Ga)Se2 solar cells," *Applied Physics Letters*, vol. 104, no. 3, Jan. 2014, Art. no. 033901, https://doi.org/10.1063/1.4862651.

[3] S. M. Ho, "Fabrication of Cu4SnS4 Thin Films: A Review," *Engineering, Technology & Applied Science Research*, vol. 10, no. 5, pp. 6161–6164, Oct. 2020, https://doi.org/10.48084/etasr.3663.

[4] C. Zhang *et al.*, "High efficiency CIGS solar cells on flexible stainless steel substrate with SiO2 diffusion barrier layer," *Solar Energy*, vol. 230, pp. 1033–1039, Dec. 2021, https://doi.org/10.1016/j.solener.2021.11.006.

[5] S. E. T. Moghaddam and S. M. Kankanani, "Numerical Simulation of a Mechanically Stacked GaAs/Ge Solar Cell," *Engineering, Technology & Applied Science Research*, vol. 7, no. 3, pp. 1611–1614, Jun. 2017, https://doi.org/10.48084/etasr.935.

[6] W. S. Liu, H. C. Hu, N. W. Pu, and S. C. Liang, "Developing flexible CIGS solar cells on stainless steel substrates by using Ti/TiN composite structures as the diffusion barrier layer," *Journal of Alloys and Compounds*, vol. 631, pp. 146–152, May 2015, https://doi.org/10.1016/j.jallcom.2014.12.189.

[7] M. D. Heinemann *et al.*, "Cu(In,Ga)Se2 superstrate solar cells: prospects and limitations," *Progress in Photovoltaics: Research and Applications*, vol. 23, no. 10, pp. 1228–1237, 2015, https://doi.org/10.1002/pip.2536.

[8] C. H. Huang, "Effects of junction parameters on Cu(In,Ga)Se2 solar cells," *Journal of Physics and Chemistry of Solids*, vol. 69, no. 2, pp. 779–783, Feb. 2008, https://doi.org/10.1016/j.jpcs.2007.07.118.

[9] A. Mavlonov *et al.*, "Superstrate-type flexible and bifacial Cu(In,Ga)Se2 thin-film solar cells with In2O3:SnO2 back contact," *Solar Energy*, vol. 211, pp. 725–731, Nov. 2020, https://doi.org/10.1016/j.solener.2020.10.019.

[10] T. Nakada, "Microstructural and diffusion properties of CIGS thin film solar cells fabricated using transparent conducting oxide back contacts," *Thin Solid Films*, vol. 480–481, pp. 419–425, Jun. 2005, https://doi.org/10.1016/j.tsf.2004.11.142.

[11] X. Li, A. Kanevce, J. V. Li, and I. Repins, "The impact of front contact ZnO:Al/Zn1-xMgxO layer on Cu(In,Ga)Se2 thin-film solar cells," *physica status solidi c*, vol. 7, no. 6, pp. 1703–1705, 2010, https://doi.org/10.1002/pssc.200983225.

[12] A. Chirilă *et al.*, "Highly efficient Cu(In,Ga)Se2 solar cells grown on flexible polymer films," *Nature Materials*, vol. 10, no. 11, pp. 857–861, Nov. 2011, https://doi.org/10.1038/nmat3122.

[13] P. Jackson, R. Wuerz, D. Hariskos, E. Lotter, W. Witte, and M. Powalla, "Effects of heavy alkali elements in Cu(In,Ga)Se2 solar cells with efficiencies up to 22.6%," *physica status solidi (RRL) – Rapid Research Letters*, vol. 10, no. 8, pp. 583–586, 2016, https://doi.org/10.1002/pssr.201600199.

[14] M. Paire, L. Lombez, J.-F. Guillemoles, and D. Lincot, "Toward microscale Cu(In,Ga)Se2 solar cells for efficient conversion and optimized material usage: Theoretical evaluation," *Journal of Applied Physics*, vol. 108, no. 3, Aug. 2010, Art. no. 034907, https://doi.org/10.1063/1.3460629.

[15] D. L. Young *et al.*, "Improved performance in ZnO/CdS/CuGaSe2 thin-film solar cells," *Progress in Photovoltaics: Research and Applications*, vol. 11, no. 8, pp. 535–541, 2003, https://doi.org/10.1002/pip.516.

[16] T. Nakada, Y. Hirabayashi, T. Tokado, D. Ohmori, and T. Mise, "Novel device structure for Cu(In,Ga)Se2 thin film solar cells using transparent conducting oxide back and front contacts," *Solar Energy*, vol. 77, no. 6, pp. 739–747, Dec. 2004, https://doi.org/10.1016/j.solener.2004.08.010.

[17] F.-J. Haug, D. Rudmann, H. Zogg, and A. N. Tiwari, "Light soaking effects in Cu(In,Ga)Se2 superstrate solar cells," *Thin Solid Films*, vol. 431–432, pp. 431–435, May 2003, https://doi.org/10.1016/S0040-6090(03)00187-1.

[18] M. D. Heinemann *et al.*, "Advantageous light management in Cu(In,Ga)Se2 superstrate solar cells," *Solar Energy Materials and Solar Cells*, vol. 150, pp. 76–81, Jun. 2016, https://doi.org/10.1016/j.solmat.2016.02.005.

[19] S. Ikeda, R. Kamai, S. Min Lee, T. Yagi, T. Harada, and M. Matsumura, "A superstrate solar cell based on $In_2(Se,S)_3$ and $CuIn(Se,S)_2$ thin films fabricated by electrodeposition combined with annealing," *Solar Energy Materials and Solar Cells*, vol. 95, no. 6, pp. 1446–1451, Jun. 2011, https://doi.org/10.1016/j.solmat.2010.11.006.

[20] M. D. Heinemann *et al.*, "The Importance of Sodium Control in CIGSe Superstrate Solar Cells," *IEEE Journal of Photovoltaics*, vol. 5, no. 1, pp. 378–381, Jan. 2015, https://doi.org/10.1109/JPHOTOV.2014.2360332.

[21] A. Mouhoub, A. Bouloufa, K. Djessas, and A. Messous, "Analytical modeling and optimization of original bifacial solar cells based on Cu(In,Ga)Se_2 thin films absorbers," *Superlattices and Microstructures*, vol. 122, pp. 434–443, Oct. 2018, https://doi.org/10.1016/j.spmi.2018.06.068.

[22] A. Mouhoub, A. Bouloufa, K. Djessas, and A. Messous, "Device modeling approach and simulation of the effect of the ODC thin layer on bifacial solar cells based on CuIn1-xGaxSe2 thin films absorbers," *Journal of Physics and Chemistry of Solids*, vol. 144, p. 109520, Sep. 2020, https://doi.org/10.1016/j.jpcs.2020.109520.

[23] A. Morales-Acevedo, N. Hernández-Como, and G. Casados-Cruz, "Modeling solar cells: A method for improving their efficiency," *Materials Science and Engineering: B*, vol. 177, no. 16, pp. 1430–1435, Sep. 2012, https://doi.org/10.1016/j.mseb.2012.01.010.

[24] C. H. Huang, "Effects of Ga content on Cu(In,Ga)Se_2 solar cells studied by numerical modeling," *Journal of Physics and Chemistry of Solids*, vol. 69, no. 2, pp. 330–334, Feb. 2008, https://doi.org/10.1016/j.jpcs.2007.07.093.

[25] I. Bouchama, K. Djessas, F. Djahli, and A. Bouloufa, "Simulation approach for studying the performances of original superstrate CIGS thin films solar cells," *Thin Solid Films*, vol. 519, no. 21, pp. 7280–7283, Aug. 2011, https://doi.org/10.1016/j.tsf.2011.01.182.

[26] A. Bouloufa, K. Djessas, and D. Todorovic, "Structural and optical properties of Cu(In,Ga)Se2 grown by close-spaced vapor transport technique," *Materials Science in Semiconductor Processing*, vol. 12, no. 1, pp. 82–87, Feb. 2009, https://doi.org/10.1016/j.mssp.2009.07.010.

[27] M. Nerat, F. Smole, and M. Topič, "A simulation study of the effect of the diverse valence-band offset and the electronic activity at the grain boundaries on the performance of polycrystalline Cu(In,Ga)Se2 solar cells," *Thin Solid Films*, vol. 519, no. 21, pp. 7497–7502, Aug. 2011, https://doi.org/10.1016/j.tsf.2010.12.100.

[28] T. B. Nasrallah, D. Mahboub, M. Jemai, and S. Belgacem, "Temperature Effect on Al/p-CuInS2/SnO2(F) Schottky Diodes," *Engineering, Technology & Applied Science Research*, vol. 9, no. 5, pp. 4695–4701, Oct. 2019, https://doi.org/10.48084/etasr.3072.